J. Fluid Mech. (1980), *vol.* 98, *part* 4, *pp.* 703–726
Printed in Great Britain

Seasonal and spring–neap tidal dependence of axial dispersion coefficients in the Severn – a wide, vertically mixed estuary

By R. J. UNCLES AND P. J. RADFORD

Natural Environment Research Council, Institute for Marine Environmental Research, Plymouth, Devon, U.K.

(Received 7 March 1979 and in revised form 22 August 1979)

Results are presented of a simplified description of the seasonal and spring–neap tidal dependence of the axial dispersion coefficients in the Severn Estuary. The coefficients are derived from salt budget calculations, which are based on 29 sets of observations of the axial salinity distributions in the estuary during 1971–1976. Regression analyses of the salinity distributions determine simple linear and logarithmic relationships for the dispersion coefficients in terms of tidal range and the total rate of input of fresh water to the estuary, the appropriate averaging periods for the freshwater inputs being computed as part of the analyses.

The results show that the coefficients generally increase with increasing run-off, and, away from the mouth, depend upon the tidal range, showing a small decrease with increasing tidal range in the seaward part of the estuary, and a large increase with increasing tidal range towards the head. The yearly averaged coefficients lie in the order-of-magnitude range 10^2–$10^3\ \mathrm{m^2\,s^{-1}}$, with the larger values occurring near the head.

The computed dispersion coefficients are applied to calculations of the seasonal dependence of residence times, the results being expressed as functions of axial distance along the estuary. It is shown that the residence time of the whole estuary varies from roughly 100 days during winter conditions to 200 days during summer conditions, and that the residence time landward of a particular section decreases rapidly as the section taken approaches the head of the estuary.

1. Introduction

An ability to predict the distributions of dissolved materials in an estuary is of considerable importance in studies of estuarine ecology and for water-quality management. The simple one-dimensional conservation of mass equation, which may be used to describe the tidally and cross-sectionally averaged mass balance of dissolved materials in estuaries, provides a useful indication of the distributions of ecological variables, and the concentrations resulting from specified discharges of contaminants into estuaries. In its simplest form (Stommel 1953; O'Connor 1962; Mollowney 1973; Boyle *et al.* 1974), this equation assumes that the local concentrations of dissolved materials depend on the degree of balance between the local source terms, the seaward transport of material due to the freshwater discharges into the estuary, and the down-gradient transport resulting from axial dispersion, with an effective axial dispersion

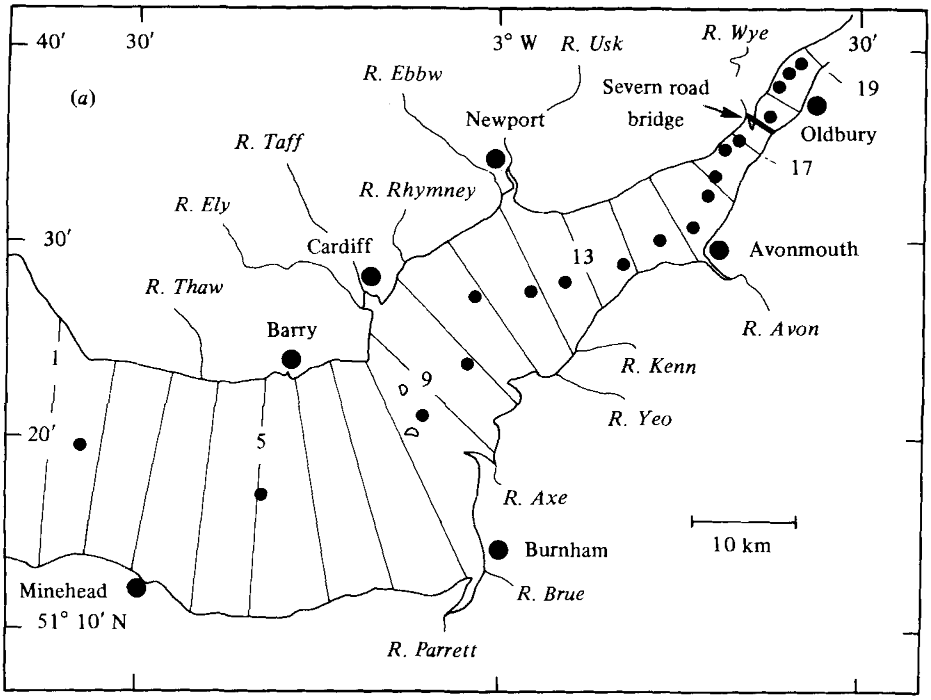

FIGURE 1 (*a*). For legend see opposite.

coefficient E ($E = DA$, where D is the dispersion coefficient, and A the estuarine cross-sectional area).

The purpose of this work is to present results for the seasonal and spring–neap tidal dependence of D in the Severn Estuary, based on observations of the axial salinity distributions during 1971–1976; results are also given for the seasonal dependence of residence times, expressed as functions of axial distance along the estuary. The work was motivated by a need to define the seasonal, long-term transport for ecological modelling studies of the Severn Estuary, although the results will also be of value to any future water quality investigations in the region; moreover, whilst these applications are essentially practical, it is considered that the results presented here will, in addition, be of value to the more theoretical studies of estuarine dispersion processes (see, for example, Fischer 1972, 1976; Smith 1977, 1980).

An evaluation of the axial dispersion coefficients in the Severn Estuary, pertinent to low freshwater run-off conditions during August 1940, has previously been made by Stommel (1953). A subsequent analysis for the same period by Bowden (1964), but for only four locations in the estuary, gave much higher values; this discrepancy can be attributed to the fact that Bowden based his calculations on a larger and more realistic estimate of the catchment area for fresh water. Time-dependent calculations of ecological variables and levels of contamination require values of D for the whole estuary, and throughout time, and the present work greatly extends these studies by computing D both as a function of the freshwater run-off into the estuary, and the spring–neap tidal range.

Sketch charts of the Severn Estuary are shown in figures 1 (*a*, *b*); figure 1 (*a*) shows

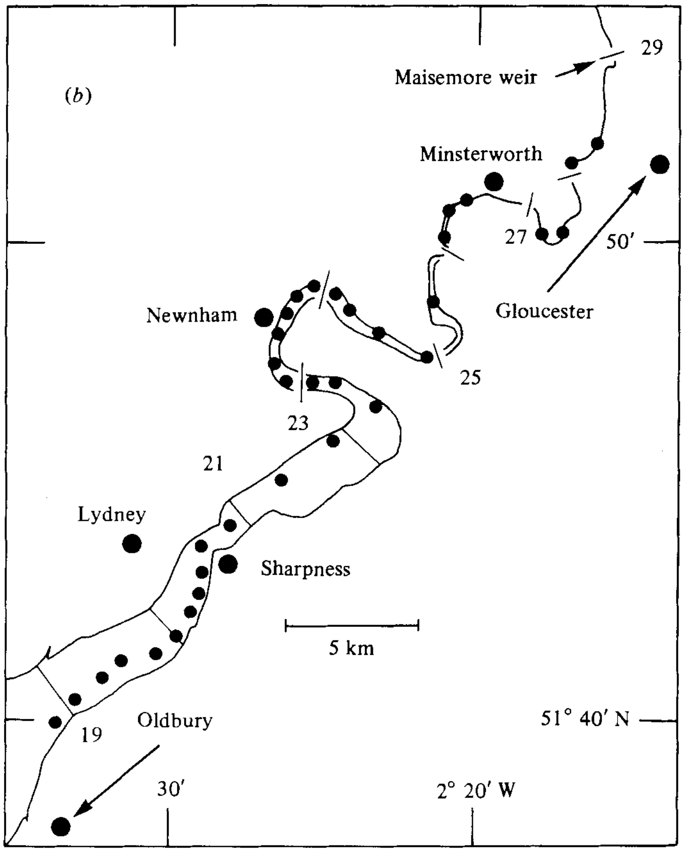

FIGURE 1. Sketch charts of the Severn Estuary. The transverse lines define a discrete representation of the estuary (k, Δx), with $\Delta x = 5$ km and with $1 \leqslant k \leqslant 29$. Locations of the major rivers entering the estuary are shown, and the stations (●) represent the sampling sites used during the helicopter surveys of 1975–1976. (*a*) Section of estuary for $1 \leqslant k \leqslant 19$, between Minehead and Oldbury. (*b*) Section of estuary for $19 \leqslant k \leqslant 29$, between Oldbury and Maisemore Weir; drawn on a larger scale than (*a*).

the section of estuary between Minehead and Oldbury, and figure 1(*b*) the section between Oldbury and Maisemore Weir. The transverse lines shown in figures 1(*a*, *b*) define a discrete (k) representation of the estuary which is used for subsequent analysis; this representation is based on Winters' work (Winters 1973). The mouth of the estuary is taken to be $k = 2$ (roughly 5 km seawards of Minehead), and the head of the estuary is taken to be $k = 29$ (Maisemore Weir); dispersion coefficients will be defined at the locations corresponding to $k = 2{\cdot}5(1)28{\cdot}5$. The stations shown in figures 1(*a*, *b*) correspond to sampling sites for salinity measurements, and will be discussed later.

Figure 2 shows the discrete (k) and continuous (x) representations of the estuary, together with associated place names. The axial distance along the estuary is given by $x = x_k = (k-29)\,\Delta x$, where $\Delta x = 5\,\text{km}$.

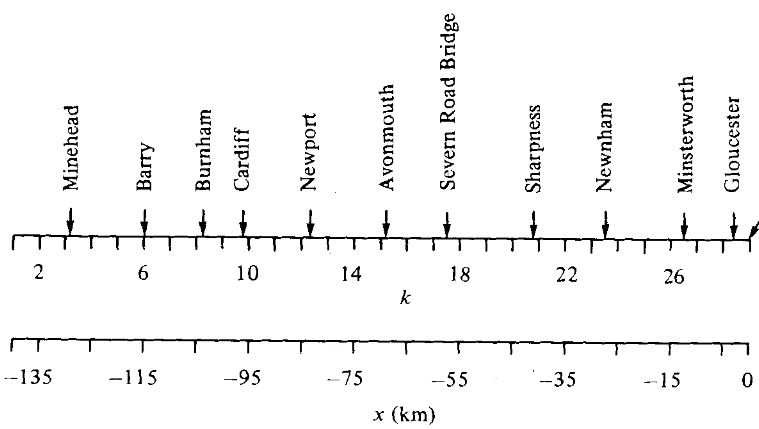

FIGURE 2. One-dimensional representation of the estuary, showing distance scale, x, and lattice scale, k.

2. Basic equations

Although this work is not principally concerned with the theoretical aspects of estuarine dispersion, it is nevertheless germane to describe those processes which contribute to the one-dimensional dispersion, in order to delineate the difficulties and uncertainties involved in defining seasonal variability from salinity data.

The salinity balance

The transport of salt and water through a fixed (Eulerian) estuarine cross-section of area A is considered. The non-turbulent component of the salinity at a position on A is denoted by s, and the corresponding value of the perpendicular, non-turbulent component of the water velocity on A by u. The instantaneous rate of transport of water across A, Q, may be written

$$Q = A\bar{u}, \tag{1}$$

where the overbar denotes an average over A. The instantaneous rate of transport of salt across A, F_s, is

$$F_s = A\overline{us} + F_{s,T}, \tag{2}$$

where F_s has units of ‰ $m^3 s^{-1} \cong kg\, s^{-1}$, and where $F_{s,T}$ is the transport due to turbulent fluctuations in salinity and velocity, which is usually considered to be small in estuaries (Pritchard 1954). The following definitions apply:

$$u = \bar{u} + u', \tag{3}$$

$$s = \bar{s} + s', \tag{4}$$

$$A = \langle A \rangle + \tilde{A}, \tag{5}$$

$$Q = \langle Q \rangle + \tilde{Q}, \tag{6}$$

$$\bar{u} = \langle \bar{u} \rangle + \tilde{u}, \tag{7}$$

and

$$\bar{s} = \langle \bar{s} \rangle + \tilde{s}, \tag{8}$$

where the primes denote a deviation from the cross-sectional average, the angle brackets denote a tidal average, and the tildes the cross-sectionally averaged tidal fluctuations. It follows from equations (3)–(8) that

$$\langle \tilde{A} \rangle = \langle \tilde{Q} \rangle = \langle \tilde{u} \rangle = \langle \tilde{s} \rangle = 0,$$

and that

$$\overline{u'} = \overline{s'} = 0.$$

The residual (tidally averaged) rate of transport of salt across A can be derived from equations (2), (3), (4), (1), (6) and (8), and is written in the form

$$\langle F_s \rangle = \langle Q \rangle \langle \bar{s} \rangle + \langle \tilde{Q}\tilde{s} \rangle + \langle A\overline{u's'} \rangle + \langle F_{s,\,T} \rangle. \tag{9}$$

The residual rate of transport of water can be separated into a part due to the freshwater inputs to the estuary landward of A, Q_f, and a part due to all other mechanisms, Q_R; that is

$$\langle Q \rangle = -Q_f + Q_R \quad \text{with} \quad Q_f \geqslant 0. \tag{10}$$

The rate of transport of salt across A determines the rate of change of the salt content of the estuary landward of A, M_s; it follows from equations (9) and (10) that

$$\frac{\partial \langle M_s \rangle}{\partial t} - Q_R \langle \bar{s} \rangle = -Q_f \langle \bar{s} \rangle + \{\langle \tilde{Q}\tilde{s} \rangle + \langle A\overline{u's'} \rangle + \langle F_{s,\,T} \rangle\}. \tag{11}$$

A coefficient of effective axial dispersion, E, is defined as follows:

$$E = -\{\langle \tilde{Q}\tilde{s} \rangle + \langle \overline{Au's'} \rangle + \langle F_{s,\,T} \rangle\}\left(\frac{\partial \langle \bar{s} \rangle}{\partial x}\right)^{-1} \quad \text{for} \quad \frac{\partial \langle \bar{s} \rangle}{\partial x} \neq 0, \tag{12}$$

and the quantity ϵ is defined by the relationship

$$\epsilon = Q_R \langle \bar{s} \rangle - \frac{\partial \langle M_s \rangle}{\partial t}. \tag{13}$$

Equation (11) becomes

$$E\frac{\partial \langle \bar{s} \rangle}{\partial x} + Q_f \langle \bar{s} \rangle = \epsilon. \tag{14}$$

An equation for the evolution of $\langle \bar{s} \rangle$ can be derived by differentiating equations (13) and (14) with respect to x, and using the results that

$$\frac{\partial M_s}{\partial x} = \frac{\partial}{\partial x}\int_x^0 A\bar{s}\,dx' = -A\bar{s}$$

and

$$\frac{\partial \langle M_s \rangle}{\partial x} = -\langle A\bar{s} \rangle = -\langle A \rangle \langle \bar{s} \rangle - \langle \tilde{A}\tilde{s} \rangle,$$

23-3

together with the tidally averaged conservation of water volume equation

$$\frac{\partial \langle A \rangle}{\partial t} = -\frac{\partial}{\partial x}\langle Q \rangle + \sum_j \langle q_j \rangle \delta(x - x_j), \tag{15}$$

in which q_j is the rate of input of fresh water at $x = x_j$, and $\delta(x - x_j)$ is the Dirac delta function. These definitions yield

$$\frac{\partial \langle \bar{s} \rangle}{\partial t} = \left[u_f \frac{\partial \langle \bar{s} \rangle}{\partial x} + \langle A \rangle^{-1} \frac{\partial}{\partial x}\left(E \frac{\partial \langle \bar{s} \rangle}{\partial x} \right) - \langle A \rangle^{-1} \langle \bar{s} \rangle \sum_j \langle q_j \rangle \delta(x - x_j) \right] - u_R \frac{\partial \langle \bar{s} \rangle}{\partial x} - \langle A \rangle^{-1} \frac{\partial}{\partial t}\langle \tilde{A}\tilde{s} \rangle, \tag{16}$$

where $u_f = Q_f / \langle A \rangle$ and $u_R = Q_R / \langle A \rangle$.

Effect of ϵ on salt balance

In equations (1)–(16) it has been assumed that the time averaging corresponds to a tidal cycle, although the same results will apply if the average is taken over 25 h, a lunar month or a year. The longer the averaging period, the smaller will be the influence of transients ($\partial \langle M_s \rangle / \partial t$) and flows, Q_R, on the salt balance; for very long periods ϵ will be negligible in equation (14) and the salt balance will be effected by the seaward advection of mean salinity resulting from freshwater flows into the estuary, and the landward diffusion of salt due to the effective axial dispersion. For shorter averaging periods, and in particular for observations extending over one or two tidal cycles, this simple balance will not apply unless

$$|\epsilon| \ll Q_f \langle \bar{s} \rangle,$$

a condition which cannot, at present, be inferred with any certainty from observations.

Uncles & Jordan (1980) have shown that the cross-sectionally averaged residual flows of water in the Severn Estuary which are generated by spring–neap variations in the tide are, on average, of the same order of magnitude as Q_f (i.e. $Q_R \sim Q_f$); it follows that estimates of the salt balance based on short-term observations will, in general, be influenced by the state of the spring–neap cycle, and concomitantly that $\epsilon \neq 0$. In addition to these tidally induced residual currents, the onset of winds will generate flows, Q_R, and influence the observed salt balance; large short-term fluctuations in Q_f will also produce transients, and render untenable the simple salt balance computed using the assumption $\epsilon = 0$.

Dispersion mechanisms

Whilst equation (12) represents a formal decomposition of the effective dispersion coefficient into separate physical mechanisms, it provides no immediate indication of which processes are likely to be dominant.

For vertically well-mixed estuaries such as the Severn (see later), a transverse eddy diffusivity of about $0{\cdot}1\ \mathrm{m^2\,s^{-1}}$ (Talbot & Talbot 1974) implies that cross-sectional mixing during one tidal period is thorough if the estuary is narrower than 100 m, and insignificant if the estuary is wider than about 500 m. Between Sharpness and Minehead (see figures 1*a*, *b*) the average width of the Severn is 14 km, and its average depth is 13 m, so that the Severn is wide in the sense that lateral diffusion due to turbulence is negligible during one tidal cycle. A recent analysis by Smith (1980) of wide, vertically well-mixed estuaries (subject to negligible Coriolis forces, curvature, lateral input and drying-bank effects) has shown that the dispersion in such model estuaries is dominated by shear processes ($\langle \overline{Au's'} \rangle$ in equation (12)), and that the appropriate non-dimensional parameters governing the dispersion are

$$\theta_0 = \Gamma\bar{h}/B, \quad \theta_1 = \bar{h}\langle|\tilde{u}|\rangle^2/B^3\omega^2\Gamma,$$

and

$$\theta_2 = (\beta g\,\partial\langle\bar{s}\rangle/\partial x)^2\bar{h}^3B\Gamma^5/\langle|\tilde{u}|\rangle^4.$$

Here $\bar{h}$ is the average depth over a cross-section of semi-width B, Γ is a non-dimensional Chezy number, ω is the frequency of the semi-diurnal tide ($1{\cdot}4 \times 10^{-4}\,\mathrm{s^{-1}}$), and βg is the reduced gravity for salt. Smith (1980) has shown that the largest of the factors θ_0, θ_1, $\theta_1^2\theta_2$ and θ_2 determines whether the dispersion is mainly due to oscillatory vertical shear, oscillatory lateral shear, the interaction between tidal and lateral buoyancy effects, or the residual buoyancy-driven lateral circulation patterns. Using typical values for the Severn

$$B \cong 7\,\mathrm{km}, \quad \bar{h} \cong 13\,\mathrm{m}, \quad \Gamma \sim 20,$$

and

$$\langle|\tilde{u}|\rangle \sim 1\,\mathrm{m\,s^{-1}}, \quad \beta g\,\partial\langle\bar{s}\rangle/\partial x \cong -2\times10^{-6}\,\mathrm{s^{-2}},$$

yields

$$\theta_0 \sim 10^{-2}, \quad \theta_1 \sim 10^{-4}, \quad \theta_1^2\theta_2 \sim 10^{-6} \quad \text{and} \quad \theta_2 \sim 10^2.$$

From the dominance of θ_2 it appears that buoyancy-driven lateral circulations are an important cause of axial dispersion in the Severn; the small contribution to the dispersion from vertical shear (small θ_0), and the importance of lateral residual circulation patterns, have also been confirmed by observations (Uncles & Jordan 1979). The efficacy of buoyancy-driven lateral circulations as a mechanism for dispersion has been demonstrated by Smith (1980) for the Thames, and by Fischer (1972, p. 684) for the Mersey, both of whom showed that in the absence of other dispersion mechanisms

$$E \propto (\partial\langle\bar{s}\rangle/\partial x)^2. \tag{17}$$

Thus, using equation (17), and assuming steady-state conditions ($\epsilon = 0$) in equation (14) (Dr R. Smith, personal communication):

$$E \propto Q_f^{\frac{2}{3}}, \tag{18}$$

neglecting the dependence of $\langle\bar{s}\rangle$ on Q_f.

3. Salinity and run-off data

Salinity data

The axial salinity distributions analysed here were derived from a number of separate experimental water quality studies of the Severn Estuary carried out during 1971–1976. Ten helicopter surveys of the estuary were made by Winters during 1971–1973 (Mr A. Winters, personal communication); these included various states of the spring–neap cycle and investigated both winter and summer conditions; results from two of these surveys have been published (Winters 1973, p. 108). In addition, three surveys of the region landward of the Severn Road Bridge (see figure 1*a*) were made during 1974 by the Severn–Trent Water Authority; the observations were made from boats situated along the central axis of the estuary, and determinations of the near-surface salinity were made at local high water. These data were complemented by near-surface measurements of salinity seaward of the Severn Road Bridge during Institute for Marine Environmental Research cruises. Finally, 16 helicopter surveys were undertaken by the Severn Estuary Technical Working Party (a consortium of Regional Water Authorities) in collaboration with IMER during 1975–1976; these surveys are still in progress, and contribute to ecological and water-quality studies of the Severn Estuary.

The majority of the data were obtained during helicopter surveys, in which the progression of high water along the estuary was followed; *in situ* measurements of the near-surface salinity, and the collection of water samples, were made at local high water for a large number of stations. Measurements of salinity were generally made using MC5 salinometers, and it is assumed that the near-surface values are representative of the whole water column; this is in accord with other investigations (Abdullah, Dunlop & Gardner 1973; Uncles & Jordan 1979), although some stratification is known to occur near the mouths of large rivers at certain states of the tide (Winters 1973, p. 108), and may occur near the head of the estuary.

The sampling grid for the helicopter surveys of 1975–1976 is shown in figures 1 (*a*, *b*), although not all of these stations were necessarily sampled on each occasion; the stations generally lie in the deeper channels. The large number of stations landward of Oldbury – see figure 1 (*b*) – is employed to accurately resolve the high gradient in salinity which is associated with the transition between saline and fresh water, and which is typically positioned between Sharpness and Maisemore Weir. The somewhat poor station resolution seaward of Burnham, figure 1 (*a*), was chosen (with hindsight) because of the difficulty of working a larger number of stations whilst following the progress of high water along the estuary. An indication of the station positions employed by the helicopter surveys of 1971–1973 is given by Winters (1973, figure 3, p. 108).

Analysis of salinity data

The observations determined s at local high water, and at positions within the main, deep channel of the estuary – which is delineated by the sampling track shown in figures 1 (*a*, *b*). Application of the data to equations (1)–(18) requires estimates of the cross-sectionally averaged salinity, and it is assumed that $s = \bar{s}$ for each observation. It is also necesssary to estimate tidal averages, $\langle \bar{s} \rangle$, from the high-water values, $\bar{s} = \bar{s}_{\mathrm{HW}}$; an approximation to $\langle \bar{s} \rangle$ has been obtained by solving numerically the equation

$$\frac{\partial \bar{s}}{\partial t} = -\tilde{u}(x, t)\frac{\partial \bar{s}}{\partial x}, \tag{19}$$

with $$\bar{s}(x, 0) = \bar{s}_{\mathrm{HW}}(x),$$

over the lattice of points $k = 1(1)29$ (see figures 1*a*, *b*), where $\tilde{u}$, the tidal velocity, is defined in equation (7). The fundamental assumption evoked by equation (19) is that the dominant variations in $\bar{s}$ within a tidal cycle are the result of tidal advection; the equation is solved by displacing $\bar{s}_{\mathrm{HW}}$ through a tidal excursion and interpolating $\bar{s}(x, t)$ to define $\bar{s}(x_k, t)$, a tidal average being formed from the computed values of $\bar{s}(x_k, t)$. Values of $\tilde{u}$ for the estuary were deduced from tidal excusion data given by Winters & Barrett (1972). It is mentioned that the amplitudes of the tidal excursions in the Severn

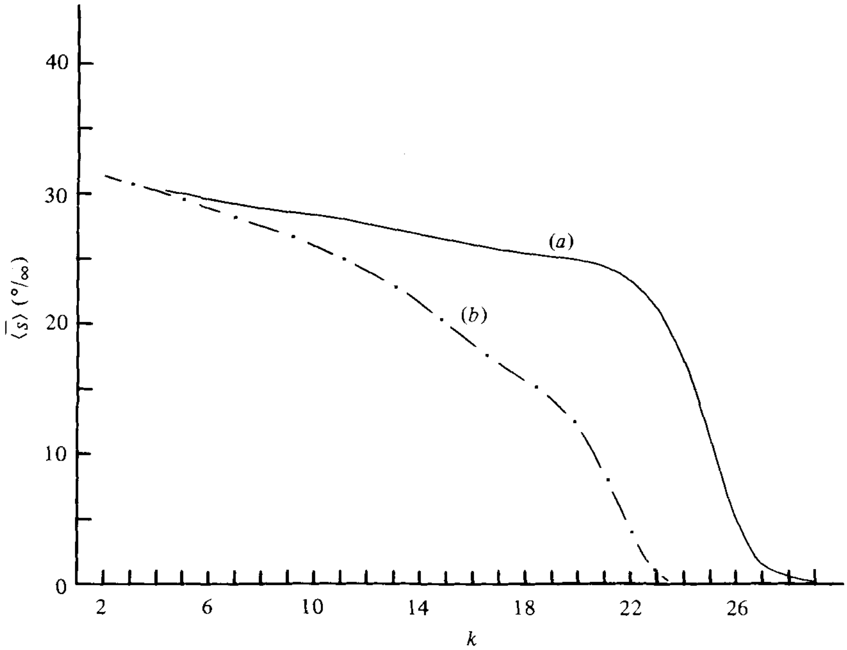

FIGURE 3. Tidally averaged salinity, $\langle \bar{s} \rangle$, for two surveys as functions of k. (a) Spring tides of June 1976, the average rate of freshwater inputs to the whole estuary for the month preceding the survey was 80 $m^3 s^{-1}$, and the tidal range at Avonmouth during the survey was 12·8 m. (b) As (a) but for neap tides of November 1976, the corresponding freshwater inputs being 480 $m^3 s^{-1}$, and the tidal range 7·3 m.

Estuary have maximum values of roughly 12 km and 6 km (approximately $2\Delta x$ and Δx) at mean spring and mean neap tides respectively, so that the effects of approximations in the evaluation of $\langle \bar{s} \rangle$ will not significantly alter the results presented here.

Some results of the procedure for calculating $\langle \bar{s} \rangle$ from $\bar{s}_{\mathrm{HW}}$ are given in figure 3; the curves shown as 'a' and 'b' represent spring-tide summer conditions, and neap-tide winter conditions respectively. The up-estuary, tidally averaged salinity increases with increasing tidal range and decreasing run-off. The large seasonal variations in $\partial \langle \bar{s} \rangle / \partial x$ will lead to variations in the buoyancy-driven circulation patterns and, in view of their apparent importance to the dispersion, to variations in E (see equations (12) and (17)). Seasonal variability in the lateral residual circulation patterns and E (through the term $\langle \overline{Au's'} \rangle$ in equation (12)) will also result from wind stress acting on the estuary, wind stress generally being stronger in the winter months. Figure 4 shows a plot of monthly-averaged surface wind stress acting on the estuary, V, against the monthly-averaged freshwater inputs to the whole estuary, $Q_{f,\,2\frac{1}{2}}$, for the years 1971–1974, as deduced from wind-speed data for Gloucester. The significant correlation between V and $Q_{f,\,2\frac{1}{2}}$ demonstrates that winter months of high run-off are also associated with stronger winds blowing over the estuary, and suggests that a seasonal description of E in terms of run-off alone will implicitly contain that component due to wind stress.

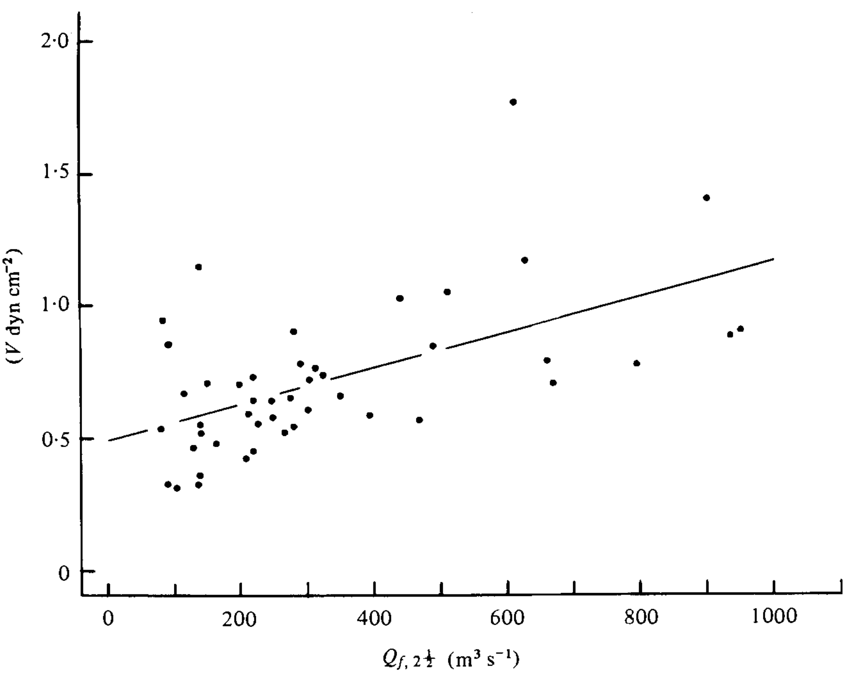

FIGURE 4. Regression of monthly-averaged wind stress (determined at Gloucester), V, with the monthly-averaged rate of freshwater inputs to the whole estuary, $Q_{f,2\frac{1}{2}}$, for the years 1971–1974. The regression line is shown, the correlation being significant at the 99·9 % confidence level with a correlation coefficient, r, of 0·57 and with 46 degrees of freedom.

Freshwater inputs

The major river systems which discharge fresh water into the Severn Estuary are shown in figures 1 (*a*, *b*); the freshwater inputs q_j, equation (15), are derived from data for the Rivers Thaw, Brue, Parrett, Axe, Taff, Ely, Rhymney, Yeo, Kenn, Usk, Ebbw, Avon and Wye. The value of $Q_f(x, t)$ is given by

$$Q_f(x,t) = \sum_j \int_x^0 \langle q_j \rangle \, \delta(x' - x_j) \, dx' + Q_f(0,t),$$

where $Q_f(0, t)$ is the freshwater input due to the River Severn, as determined at Gloucester. The long-term yearly-averaged rate of input of fresh water to the whole estuary from the rivers amounts to approximately 300 m^3 s^{-1} (Winters 1973, p. 108), of which roughly 60 % is due to the Rivers Severn and Wye; the River Usk contributes roughly 15 % of the yearly-averaged discharges.

An additional source of fresh water to the Severn Estuary is rainfall over its surface area. Calculations of the excess of rainfall over evaporation have not been made, although a rough estimate has been derived from data given by Bowden (1955, table 19, p. 50), who computed a value of 22·4 cm year^{-1} for the excess of rainfall over evaporation in the Irish Sea; assuming that this result is applicable to the Severn Estuary, then the additional annual freshwater inputs due to this mechanism amount to less than 1 % of the inputs due to the rivers for the region landward of Burnham (figure 1 *a*), and less than 3 % for the region landward of Minehead. These inputs were therefore neglected in view of their comparative insignificance.

4. Dispersion coefficients

The effective dispersion coefficient, E, is immediately applicable to water-quality studies, although the dispersion coefficient, D, is of more physical interest, and may be easily compared for different estuaries (Dyer 1974); D is defined here by the relationship

$$D = E/A',$$

where A' is the long-term time-averaged cross-sectional area of the estuary, so that temporal variations in D are directly related to those in E. It follows from equation (14) that

$$D = Q_f F + \epsilon \left[A' \frac{\partial \langle \bar{s} \rangle}{\partial x} \right]^{-1}, \tag{20}$$

where

$$F = -\langle \bar{s} \rangle . \left[A' \frac{\partial \langle \bar{s} \rangle}{\partial x} \right]^{-1}. \tag{21}$$

Here $\langle \bar{s} \rangle$ is the observed salinity distribution averaged over a single tidal cycle, so that ϵ will not generally be negligible in equation (20), nor can it be estimated with any certainty from the data; however, to proceed it is necessary to make assumptions regarding the nature of ϵ. Considering zero wind stress and unvarying periodic tides, the variations in D will, according to equation (12), depend mainly on the variations in salinity resulting from unsteady freshwater inputs; changes in the dispersion will therefore occur on the same time-scale as those for salinity, whereas the advective transport, $-Q_f . \langle \bar{s} \rangle$, will change according to the daily fluctuations in Q_f. If $\langle \bar{s} \rangle$ is a function of Q_f^* (the average run-off into the estuary over the preceding d^* days) then D and F will also be functions of Q_f^*, and equation (20) may be written

$$D = Q_f^* F(Q_f^*) + \left[A' \frac{\partial \langle \bar{s} \rangle}{\partial x} \right]^{-1} . [\epsilon - \langle \bar{s} \rangle (Q_f - Q_f^*)].$$

For the case of zero wind stress and unvarying periodic tides ($Q_R = 0$ in equation (13)) it is assumed that

$$\epsilon = \langle \bar{s} \rangle (Q_f - Q_f^*),$$

which removes short-term variations and ensures that D varies on the same time scale as $\langle \bar{s} \rangle$, so that

$$D = Q_f^* F(Q_f^*). \tag{22}$$

Considering zero wind stress and constant freshwater inputs ($Q_f = Q_f^*$), equation (12) shows that variations in D depend on the variations in tidal flow, and can be related to the tidal states pertaining during the periods of observations. Each observation of D (computed from the data using equation (22)) will differ from the true value of D by an amount proportional to ϵ, whose influence can be minimized by combining data which cover a wide range of tidal states within which ϵ may be considered randomly distributed.

The direct effects of wind stress on the dispersion are not amenable to analysis; however, the short-term random fluctuations in wind stress will presumably be removed by the combination of data. The correlation between wind stress and run-off when viewed on a seasonal basis is shown in figure 4, and although it seems likely that wind-driven circulation may have an effect on dispersion which is physically independent of run-off, it is assumed that a description of the seasonal variability of D in terms of Q_f^* will implicitly contain that component which is due to wind stress.

Linear regression analyses

A linear model for D is chosen of the form

$$D_{k+\frac{1}{2}} = D_{1,k+\frac{1}{2}}(R-\hat{R}) + D_{2,k+\frac{1}{2}}(Q^*_{f,2\frac{1}{2}} - \hat{Q}_f) + D_{3,k+\frac{1}{2}} \quad \text{for} \quad D_{k+\frac{1}{2}} \geqslant 0 \tag{23}$$

with $\hat{Q}_f = 300\,\text{m}^3\,\text{s}^{-1}$ and $\hat{R} = 9{\cdot}4\,\text{m}$.

Here R is the range of the vertical tide at Avonmouth, and $\hat{R}$ is the long-term mean value of R (Admiralty Tide Tables 1978); $Q^*_{f,2\frac{1}{2}}$ is the total rate of input of fresh water to the estuary averaged over the preceding d^* days, computed at $k = 2\frac{1}{2}$, and D_1, D_2 and D_3 are functions of k only. Possible negative values of $D_{k+\frac{1}{2}}$ are replaced by $D_{k+\frac{1}{2}} \equiv 0$.

The advantages of defining D from equation (23) are the reduction of all the results to the definitions of D_1, D_2 and D_3, the reduction in random errors resulting from the aggregation of data, and the ease with which equation (23) can be incorporated into ecological and water models – $Q^*_{f,2\frac{1}{2}}$ and R being sufficient exogenous data to define D in the one-dimensional conservation of mass equation. A similar approach to the determination of D, although excluding the tidal dependence, was used by O'Connor (1962) for New York Harbor, and Williams & West (1973) for the Tay Estuary. A further advantage accruing from the use of a linear model is that average values of D over arbitrary periods, T, can be easily defined because of the result

$$\frac{1}{T}\int D(Q^*_{f,2\frac{1}{2}}, R)\,dt = D\left(\frac{1}{T}\int Q^*_{f,2\frac{1}{2}}\,dt, \frac{1}{T}\int R\,dt\right). \tag{24}$$

The coefficients in equation (23) are determined from multiple-regression analyses of F (see equation (21)) in the form

$$F_{k+\frac{1}{2}} = F_{1,k+\frac{1}{2}}(R-\hat{R})/Q^*_{f,2\frac{1}{2}} + F_{2,k+\frac{1}{2}}/Q^*_{f,2\frac{1}{2}} + F_{3,k+\frac{1}{2}}, \tag{25}$$

which parametrizes the observed salinity distributions in terms of tidal range and the average freshwater inputs over d^* days preceding the observations; this procedure is valid statistically because $(R-\hat{R})/Q^*_{f,2\frac{1}{2}}$ and $1/Q^*_{f,2\frac{1}{2}}$ are independent variables. The quantity d^* is evaluated by performing the analyses for 1, 3, 7, 14, 21 and 30(30)180 day averaging periods, and choosing that period which maximizes the correlation coefficient; therefore, on average, F depends most strongly on the run-off into the estuary over the preceding d^* days. The individual river inputs are strongly correlated with each other, and to a good approximation it may be shown that

$$Q^*_{f,k+\frac{1}{2}} = \alpha_{k+\frac{1}{2}} Q^*_{f,2\frac{1}{2}} \quad \text{for} \quad 1 \geqslant \alpha_{k+\frac{1}{2}} > 0. \tag{26}$$

Combining equations (22), (25) and (26) gives equation (23) with

$$D_{1,k+\frac{1}{2}} = \alpha_{k+\frac{1}{2}} F_{1,k+\frac{1}{2}}, \quad D_{2,k+\frac{1}{2}} = \alpha_{k+\frac{1}{2}} F_{3,k+\frac{1}{2}} \quad \text{and} \quad D_{3,k+\frac{1}{2}} = \alpha_{k+\frac{1}{2}}[F_{2,k+\frac{1}{2}} + \hat{Q}_f F_{3,k+\frac{1}{2}}].$$

Results of analyses

Table 1 shows the results of the multiple regression analyses for F (equation (25)). The correlation coefficients (r) for the regressions are shown, together with the associated

k	F_1 ($\mathrm{m\,s^{-1}}$)	F_2 ($\mathrm{m^2\,s^{-1}}$)	F_3 ($\mathrm{m^{-1}}$)	r	Degrees of freedom	d^* (days)
2·5	-3 ± 2	50 ± 10	$0·36 \pm 0·07$	0·80	21	60
3·5	3 ± 2	50 ± 10	$0·36 \pm 0·07$	0·79	21	60
4·5	4 ± 2	50 ± 10	$0·44 \pm 0·08$	0·77	21	60
5·5	1 ± 2	60 ± 10	$0·43 \pm 0·08$	0·79	21	60
6·5	-9 ± 3	70 ± 15	$0·56 \pm 0·11$	0·76	23	60
7·5	-19 ± 5	95 ± 20	$0·73 \pm 0·14$	0·80	24	60
8·5	-7 ± 5	170 ± 20	$0·54 \pm 0·14$	0·89	24	60
9·5	-9 ± 6	200 ± 25	$0·54 \pm 0·20$	0·85	25	60
10·5	-16 ± 6	200 ± 25	$0·36 \pm 0·20$	0·88	25	30
11·5	-16 ± 5	230 ± 20	$0·04 \pm 0·17$	0·93	26	30
12·5	-10 ± 4	220 ± 15	$0·29 \pm 0·13$	0·95	26	21
13·5	0 ± 5	300 ± 20	$0·37 \pm 0·20$	0·94	26	21
14·5	1 ± 6	330 ± 20	$0·52 \pm 0·21$	0·95	26	14
15·5	19 ± 6	380 ± 20	$0·67 \pm 0·24$	0·96	25	14
16·5	15 ± 7	530 ± 30	$0·90 \pm 0·27$	0·97	25	14
17·5	6 ± 28	1600 ± 100 (1500 ± 100)	$-1·5 \pm 1·1$ (0)	0·95	24	14
18·5	35 ± 36	1900 ± 100 (1700 ± 100)	$-2·9 \pm 1·4$ (0)	0·95	22	14
19·5	110 ± 40	1400 ± 200 (1300 ± 100)	$-1·7 \pm 1·8$ (0)	0·90	21	3
20·5	120 ± 60	2000 ± 200 (1550 ± 150)	$-5·7 \pm 2·4$ (0)	0·91	21	3
21·5	240 ± 30	550 ± 100	$1·7 \pm 1·3$	0·91	21	3
22·5	300 ± 35	370 ± 130	$3·5 \pm 1·4$	0·91	21	3
23·5	510 ± 70	440 ± 260	$7·8 \pm 3·0$	0·89	18	3
24·5	320 ± 60	180 ± 220	$8·5 \pm 2·9$	0·87	10	3

TABLE 1. Multiple regression analysis of F. Regression coefficients F_1, F_2 and F_3 (defined in equation (25)) are tabulated as functions of k, together with the correlation coefficients, r, and the degrees of freedom. The quantity d^* is the averaging period for the freshwater inputs, which is chosen to maximize r for each value of k. Also shown for $17·5 \leqslant k \leqslant 20·5$, and enclosed in parentheses, are regression relationships which are constrained to satisfy $F_3 = 0$.

degrees of freedom. The degrees of freedom decrease towards the mouth of the estuary because not all the surveys extended to the seaward boundary, and decrease towards the head because of the frequent occurrence of very-low-salinity water (< 1 ‰) in this region, which precludes the presentation of results for $k > 24·5$. The correlations are significant at the 99·9 % confidence level, which justifies the use of the simple representation defined by equation (25); the correlation coefficients maximize for values of d^* which decrease from 60 days near the mouth to three days near the head (table 1).

The errors shown in table 1 for F_1, F_2 and F_3 are standard errors computed from the regression analyses. The negative values of F_3 which occur for $17·5 \leqslant k \leqslant 20·5$ (between the Severn Road Bridge and Sharpness) are not significantly different from zero (one-tail Student-t test), and are unreasonable physically because they imply that $F < 0$ for sufficiently large values of Q_f^*, which is not observed; these regressions were therefore recomputed for the case in which F_3 was constrained to be zero, and the associated values of F_2 are listed in table 1.

The values of α used in equation (26) are listed in table 2, and are based on the mean of data for river inputs for the period 1971–1976; also given in table 2 are the long-term mean cross-sectional areas of the estuary, A' (derived from data supplied by

k	α	A' (10^3 m^2)	D_1 (m s^{-1})	D_2 (m^{-1})	D_3 (m^2 s^{-1})
2·5	1·00	460	-3 ± 2	$0{\cdot}36 \pm 0{\cdot}07$	160 ± 20
3·5	1·00	450	3 ± 2	$0{\cdot}36 \pm 0{\cdot}07$	160 ± 20
4·5	0·97	420	4 ± 2	$0{\cdot}43 \pm 0{\cdot}08$	180 ± 20
5·5	0·97	390	0 ± 2	$0{\cdot}42 \pm 0{\cdot}08$	180 ± 20
6·5	0·97	360	-9 ± 3	$0{\cdot}54 \pm 0{\cdot}11$	230 ± 20
7·5	0·97	310	-18 ± 5	$0{\cdot}71 \pm 0{\cdot}14$	300 ± 30
8·5	0·88	260	-6 ± 4	$0{\cdot}48 \pm 0{\cdot}12$	300 ± 30
9·5	0·87	220	-8 ± 5	$0{\cdot}47 \pm 0{\cdot}17$	320 ± 40
10·5	0·78	180	-12 ± 5	$0{\cdot}28 \pm 0{\cdot}16$	240 ± 40
11·5	0·77	140	-12 ± 4	$0{\cdot}03 \pm 0{\cdot}13$	180 ± 30
12·5	0·62	110	-6 ± 2	$0{\cdot}18 \pm 0{\cdot}08$	190 ± 20
13·5	0·62	74	0 ± 3	$0{\cdot}23 \pm 0{\cdot}12$	260 ± 30
14·5	0·62	56	1 ± 4	$0{\cdot}32 \pm 0{\cdot}13$	300 ± 30
15·5	0·57	43	11 ± 3	$0{\cdot}38 \pm 0{\cdot}14$	330 ± 30
16·5	0·57	30	9 ± 4	$0{\cdot}51 \pm 0{\cdot}15$	460 ± 30
17·5	0·35	21	2 ± 10	0	510 ± 30
18·5	0·35	13	12 ± 13	0	590 ± 30
19·5	0·35	9·2	39 ± 14	0	460 ± 40
20·5	0·35	5·9	42 ± 21	0	540 ± 50
21·5	0·35	3·7	84 ± 11	$0{\cdot}6 \pm 0{\cdot}5$	370 ± 100
22·5	0·35	2·0	100 ± 12	$1{\cdot}2 \pm 0{\cdot}5$	490 ± 120
23·5	0·35	0·67	180 ± 20	$2{\cdot}7 \pm 1{\cdot}1$	970 ± 240
24·5	0·35	0·53	110 ± 20	$3{\cdot}0 \pm 1{\cdot}0$	960 ± 250
25·5	0·35	0·36	190	3·9	1240
26·5	0·35	0·20	210	4·5	1420
27·5	0·35	0·12	230	4·9	1530
28·5	0·35	0·15	250	5·4	1620

TABLE 2. Dispersion coefficients for the Severn Estuary. D_1, D_2 and D_3 (defined in equation (23)) are tabulated as functions of k together with the values of α (equation (26)) used in the calculations, and the mean cross-sectional areas of the estuary A'. The coefficient D is computed according to $F_3 = 0$ (table 1) for $17{\cdot}5 \leqslant k \leqslant 20{\cdot}5$, and values for $k \geqslant 25{\cdot}5$ are subjective estimates.

Mr A. Winters, personal communication) and the computed values of D_1, D_2 and D_3 with their associated standard errors (see equation (23)). Values of D_2 and D_3 for $17{\cdot}5 \leqslant k \leqslant 20{\cdot}5$ assume that $F_3 = 0$. The quantities F and A' (tables 1 and 2), together with equations (21) and (25), parametrize the salinity distribution in the Severn Estuary relative to its value at the mouth.

The values of D_1, D_2 and D_3 shown in table 2 for $k > 24{\cdot}5$ were derived by subjective smoothing of the data for $k \leqslant 24{\cdot}5$, and extrapolating the smoothed values to the head; these subjective values are included in order to specify D for the whole estuary, which is necessary if modelling studies are to use the 'natural' barrier at Maisemore Weir as their landward boundary (although large spring tides can influence the region landward of the weir).

The dispersion coefficient D_3 (table 2), for the estuary under average conditions of tidal range and freshwater inputs, is also the long-term mean dispersion coefficient for the estuary in view of the linearity condition, see equation (24), and lies in the order-of-magnitude range 10^2–10^3 m^2 s^{-1}, with the larger values occurring near the head. The results can be compared with values of 5000 m^2 s^{-1} for the Columbia River, 24 m^2 s^{-1}

for the James River, 161–360 $m^2 s^{-1}$ for the Mersey, 158 $m^2 s^{-1}$ for Southampton Water, 50–300 $m^2 s^{-1}$ for the Tay and 53–338 $m^2 s^{-1}$ for the Thames (see Dyer 1974, and the references cited therein). The accuracy of the determinations deteriorates landward of Sharpness ($k = 20{\cdot}5$), which corresponds approximately with the position at which mean sea level intersects the estuary's bed; this landward region experiences the largest fluctuations in salinity due to variations in the tidal range and freshwater inputs, and it is not surprising that the definition of mean dispersion coefficients is less certain here than for the seaward regions. It is interesting to note that the seaward maximum in D_3 occurs near Burnham ($k = 8{\cdot}5$), and may be associated with the strong lateral current shear which results from the high curvature of the estuary in this region, see figure 1 (*a*).

The values of D_1 in table 2 define the dependence of the dispersion on tidal range (equation (23)); the errors are generally large, but the data nevertheless demonstrate important features of the tidally induced variability. D_1 is not significantly different from zero seaward of Barry ($k < 6$), showing that spring–neap variations have negligible influence on the axial distribution of salinity. D_1 is negative between Barry and Newport ($k = 12{\cdot}5$); that is, the dispersion is larger at neap tides than at spring tides, other conditions being held constant. It is suggested that the reduced dispersion at spring tides is a result of increased cross-sectional mixing and strong lateral residual currents, which are generated by centrifugal effects due to the estuary's curvature, and which provide greater lateral homogeneity.

The dispersion coefficient D_1 is positive landward of Newport ($k > 12{\cdot}5$), and rapidly increases landward of Oldbury ($k \geqslant 18{\cdot}5$). The rapid increase is partly due to changes in the tidally averaged volume of this section of estuary during a spring–neap cycle, the volume maximizing for spring tides and minimizing for neap tides (Uncles & Jordan 1980); water in the landward section of estuary is more saline at spring tides, and this appears in the one-dimensional analysis as an increase in the axial dispersion.

The seasonal (run-off) dependence of the axial dispersion coefficient is defined by D_2 in table 2 (see equation (23)). The results are reasonably accurate for the region seaward of Burnham ($k \leqslant 8{\cdot}5$), and show that the axial dispersion is larger during high run-off winter conditions than during low run-off summer conditions. Landward of Burnham the errors are larger, although the general indication is of an increase in D with increasing run-off. The dependence of D on run-off can be understood qualitatively if, as appears to be the case from theoretical considerations, buoyancy-driven horizontal circulations play an important role in the axial dispersion (Smith 1980; Fischer 1972; p. 684); when this mechanism dominates, equation (18) is approximately true for steady conditions in the absence of significant Coriolis, curvature, lateral input or drying-bank effects. The additional seasonal variability in the axial dispersion due to wind-induced transverse shear cannot be separated from that due to run-off in this analysis.

Some results of applying the data in table 2 to equation (23) are shown in figures 5 (*a–c*). Figure 5 (*a*) shows D_3, and figure 5 (*b*) shows D for average tidal conditions ($R = \hat{R}$), and for $Q^*_{f,2\frac{1}{2}} = 0$ and $10^3\ m^3 s^{-1}$ (shown as (i) and (ii) respectively). The curve drawn in figure 5 (*a*) is used to define D_3 for $k > 24{\cdot}5$; spatial smoothing of D_1, D_2 and D_3 could be used to make D a smooth function of k for all values of $Q^*_{f,2\frac{1}{2}}$ and R, but there seems little physical justification for doing this. The result for $Q^*_{f,2\frac{1}{2}} = 0$ ((i) in figure 5 (*b*)) is the 'background' dispersion coefficient for the estuary, and, except around

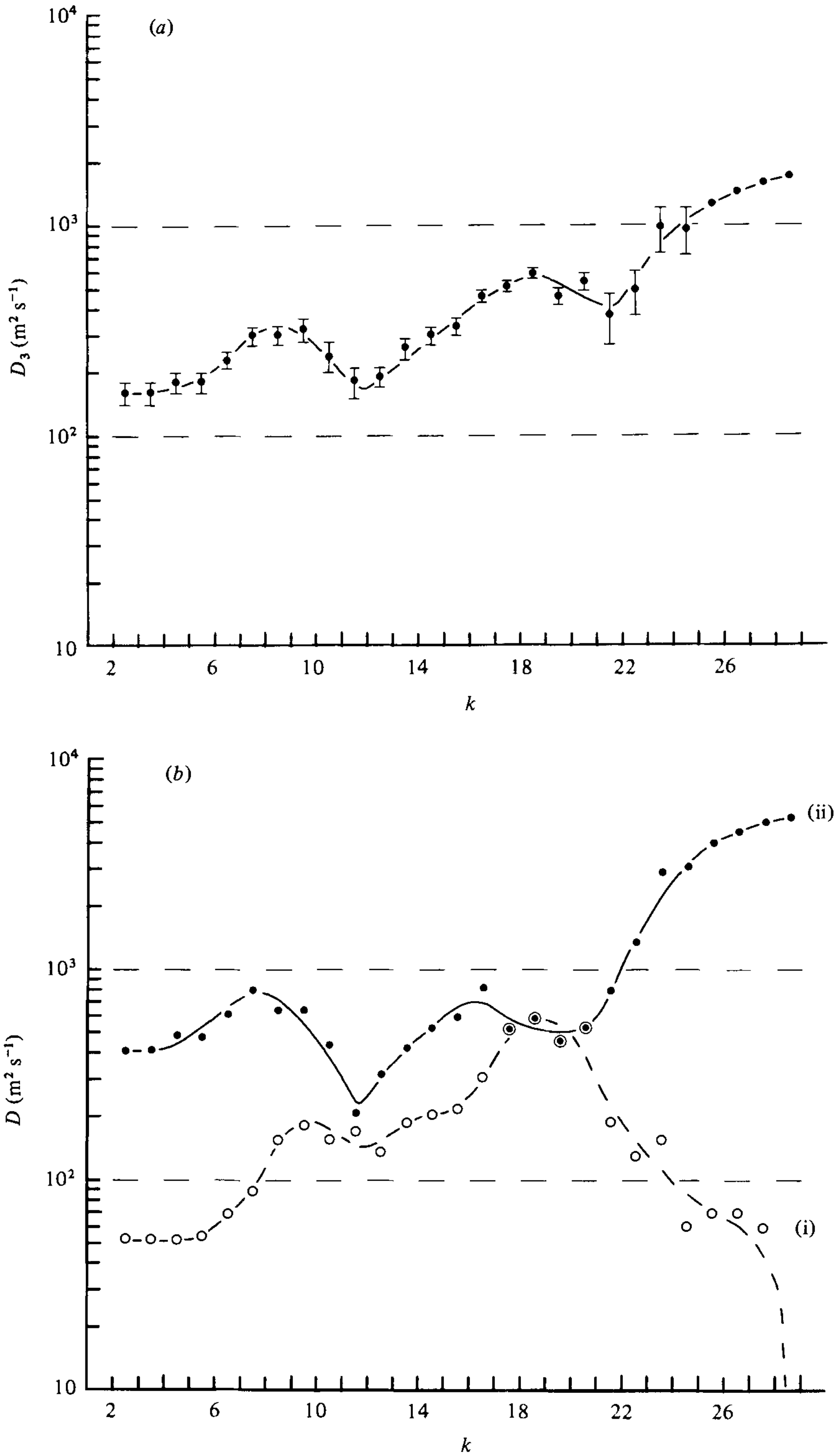

FIGURE 5 (*a*), (*b*). For legend see opposite.

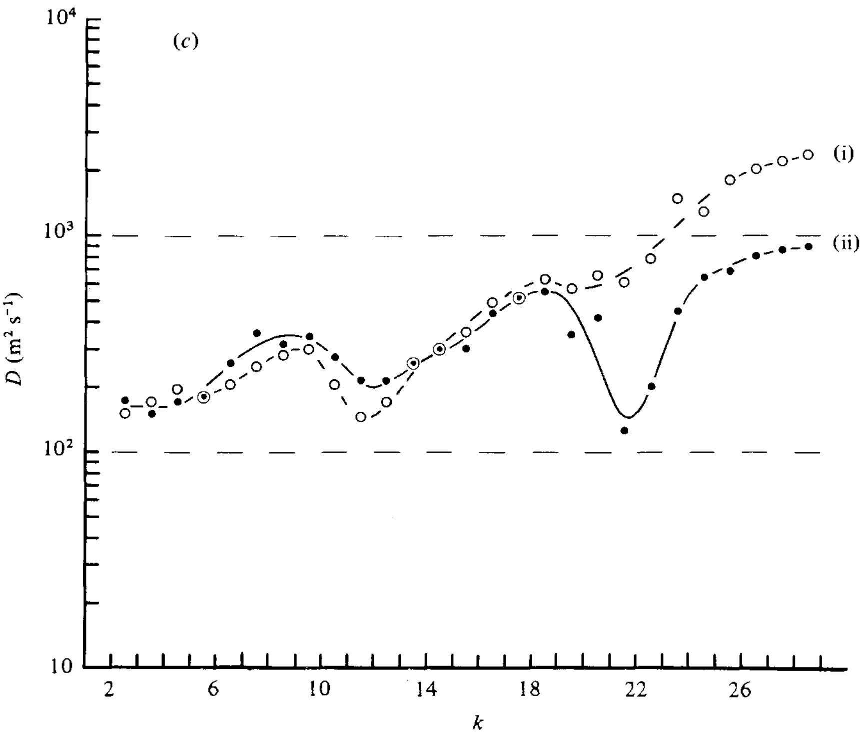

FIGURE 5. Dispersion coefficients, D, as functions of k for various values of the freshwater inputs and tidal range. The curves are subjectively smoothed representations of the data, and are included to facilitate the visual presentation of results. (*a*) D_3 against k, the error bars being drawn from data in table 2. (*b*) D against k for $R = \hat{R}$. (i) ○, $Q^*_{f,2\frac{1}{2}} = 0$. (ii) ●, $Q^*_{f,2\frac{1}{2}} = 10^3 \mathrm{m^3 s^{-1}}$. (*c*) D against k for $Q^*_{f,2\frac{1}{2}} = \hat{Q}_f$. (i) ○, $R = 12{\cdot}3$ m (mean spring tides). (ii) ●, $R = 6{\cdot}5$ m (mean neap tides).

$k = 19$, is generally much smaller than that pertaining during high run-off conditions.

Figure 5 (*c*) shows D as a function of k for $Q^*_{f,2\frac{1}{2}} = \hat{Q}_f$ (average freshwater inputs) and with the tidal range equal to that at mean spring and mean neap tides ((i) and (ii) respectively). These values are again taken from the data in table 2, and demonstrate that the major differences between neap and spring tides occur in the region $k > 20{\cdot}5$ (landward of Sharpness). The minimum in D near Sharpness is very pronounced for neap tides ((ii) in figure 5 (*c*)), and approaches zero as $Q^*_{f,2\frac{1}{2}}$ becomes small; for $Q^*_{f,2\frac{1}{2}}$ less than $130\,\mathrm{m^3 s^{-1}}$ the landward dispersive flux of salt near Sharpness is zero for mean neap tides.

Logarithmic regression analyses

Equation (23) delineates the essential behaviour of D with tidal state and run-off, and also provides a quantitative description of D for modelling studies; however, the significant dependence of D on run-off indicates strong buoyancy effects, and from a fundamental viewpoint it is of interest to see whether the data can be approximated by a relationship of the form of equation (18) in some stretches of the estuary.

The logarithmic analogue of equation (23) yields a regression equation for D of the form

$$D = d_3 . (R/\hat{R})^{d_1} . (Q^*_{f,2\frac{1}{2}}/\hat{Q}_f)^{d_2}, \tag{27}$$

k	r	Degrees of freedom	d_1	d_2	d_3 ($m^2 s^{-1}$)	H
2·5	0·72	21	$-0·1 \pm 0·2$	$0·63 \pm 0·08$	160 ± 10	A
3·5	0·77	21	$0·2 \pm 0·2$	$0·59 \pm 0·07$	160 ± 10	A
4·5	0·79	21	$0·3 \pm 0·2$	$0·60 \pm 0·07$	180 ± 10	A
5·5	0·83	21	$0·2 \pm 0·2$	$0·55 \pm 0·07$	180 ± 10	A
6·5	0·82	23	$-0·5 \pm 0·2$	$0·53 \pm 0·08$	210 ± 10	A
7·5	0·83	24	$-0·7 \pm 0·2$	$0·50 \pm 0·08$	270 ± 20	R
8·5	0·83	24	$-0·3 \pm 0·2$	$0·42 \pm 0·08$	290 ± 20	R
9·5	0·84	25	$-0·4 \pm 0·2$	$0·35 \pm 0·09$	310 ± 20	R
10·5	0·88	25	$-0·6 \pm 0·2$	$0·30 \pm 0·08$	240 ± 20	R
11·5	0·90	26	$-0·6 \pm 0·2$	$0·31 \pm 0·07$	210 ± 10	R
12·5	0·92	26	$-0·4 \pm 0·2$	$0·31 \pm 0·06$	210 ± 10	R
13·5	0·93	26	$-0·5 \pm 0·2$	$0·15 \pm 0·07$	250 ± 20	R
14·5	0·96	26	$0·1 \pm 0·1$	$0·20 \pm 0·05$	300 ± 10	R
15·5	0·95	25	$0·3 \pm 0·2$	$0·25 \pm 0·05$	340 ± 20	R
16·5	0·95	25	$0·3 \pm 0·2$	$0·22 \pm 0·05$	460 ± 20	R
17·5	0·93	24	$0·1 \pm 0·3$	$0·00 \pm 0·08$	450 ± 40	R
18·5	0·90	22	$0·5 \pm 0·3$	$0·02 \pm 0·10$	490 ± 50	R
19·5	0·81	21	$1·0 \pm 0·4$	$0·21 \pm 0·14$	450 ± 70	R
20·5	0·81	21	$1·8 \pm 0·5$	$0·17 \pm 0·16$	380 ± 70	R
21·5	0·86	21	$2·3 \pm 0·4$	$0·49 \pm 0·12$	350 ± 40	A
22·5	0·85	21	$2·5 \pm 0·4$	$0·73 \pm 0·12$	440 ± 50	A
23·5	0·82	18	$2·4 \pm 0·4$	$0·77 \pm 0·12$	830 ± 110	A
24·5	0·67	10	$1·4 \pm 0·6$	$0·75 \pm 0·15$	890 ± 170	A

TABLE 3. Dispersion coefficients for the Severn Estuary. The coefficients d_1, d_2 and d_3 (defined in equation (27)) are tabulated as functions of k, together with the correlation coefficients for the logarithmic regressions, r, and the degrees of freedom. H shows the results of a Student-t test for the hypothesis $d_2 = \frac{2}{3}$.

where the analyses are performed on F (see equation (21)), and where D is deduced from equation (22). The results for d_1, d_2 and d_3 (equation (27)) are given in table 3, together with the correlation coefficients, r, and the degrees of freedom; also shown are the results of a student-t test, H, of the hypothesis (see equation (18))

$$d_2 = \tfrac{2}{3},$$

the test concluding that there is either insufficient (A) or sufficient (R) evidence to reject the hypothesis at the 95 % level of significance.

Table 3 shows that d_2 is significantly different from $\frac{2}{3}$ for $6·5 < k < 21·5$, so that equation (18) is not valid for most of the estuary; however, the results indicate that buoyancy effects are generally important, although they do not influence the dispersion as strongly as is indicated by equation (18), perhaps as a consequence of Coriolis effects, or (as is more likely) the generation of nonlinear tidal residual currents due to channel and coastline curvature, and the effects of lateral inputs of fresh water.

The logarithmic regressions yield positive values of d_2 for all k, which further justifies the artefact of putting $D_2 \equiv 0$ for $17·5 \leqslant k \leqslant 20·5$ in table 2; in addition, a comparison of tables 2 and 3 shows that d_3 is not significantly different from D_3.

5. Residence times

The residence time (or flushing time) is a useful and widely used measure of the time-scale for retention of fresh water and conservative dissolved materials in estuaries. The residence time, τ, for the section of estuary $0 > x > x'$ is usually defined by (Hamilton 1973, p. 415)

$$\int_{t-\tau}^{t} Q_f(x', t')\, dt' = W(x', t), \tag{28}$$

where $W(x', t)$ is the freshwater content of the estuary landward of $x = x'$. Equation (28) is clearly a pseudo-steady-state approximation in which $W(x', t)$ is assumed to be essentially constant over the time τ. In the opposite extreme, of drought conditions say, an alternative definition for τ would be as the decay time-scale for the freshwater content to reduce by a factor of $1/e$. A reasonable first-order decay equation for W, which is consistent with both these extremes, is

$$\frac{\partial W(x', t)}{\partial t} = \dot{W} = Q_f(x', t) - \frac{W(x', t)}{\tau(x', t)}. \tag{29}$$

Thus, the rate of removal of fresh water from the section of estuary $0 > x > x'$ is modelled as depending upon (W/τ) rather than upon the complex local processes (cf. equation (11)).

The time τ has been computed on a seasonal basis for the Severn Estuary by solving equation (16) on the lattice of points shown in figures 1 (a, b); the two-step Lax–Wendroff scheme is used (Richtmyer & Morton 1967, p. 303), and it is assumed that $Q_R = 0$, $R = \hat{R}$ and $|\partial \langle \tilde{A}\tilde{s}\rangle/\partial t| \ll |\langle A\rangle\, \partial \langle \bar{s}\rangle/\partial t|$ for the purposes of computing seasonal variability. The boundary condition at Maisemore Weir is $\langle \bar{s}\rangle_{29} = 0$, and a good approximation to the seaward boundary condition may be written:

$$\langle \bar{s}\rangle_2 = 32{\cdot}5/[1 + (1{\cdot}28 \times 10^{-4} Q^*_{f,2\frac{1}{2}})], \tag{30}$$

which is valid for the observed range of values assumed by $Q^*_{f,2\frac{1}{2}}$ (the averaged rate of input of fresh water to the estuary over the preceding 60 days). Equation (30) implies that $\langle \bar{s}\rangle_2$ approaches 32·5 ‰ as $Q^*_{f,2\frac{1}{2}}$ tends to zero, although of course, in the hypothetical situation of no freshwater flow into the Bristol Channel and Severn Estuary over a long period, $\langle \bar{s}\rangle_2$ would assume the salinity of the North East Celtic Sea (approximately 35 ‰).

The freshwater content of the estuary is defined from the relationship

$$W_{k+\frac{1}{2}} = \sum_{k+1}^{29} A'_{k'} \Delta x (1 - \langle \bar{s}\rangle_{k'}/35) - \tfrac{1}{2} A'_{29} \Delta x$$

and τ is computed from equation (29) in the form

$$\tau_{k+\frac{1}{2}} = W_{k+\frac{1}{2}}/(Q_{f,k+\frac{1}{2}} - \dot{W}_{k+\frac{1}{2}}).$$

The monthly-averaged freshwater inputs to the estuary from each river are averaged, month by month, for the years 1971–1976, in order to derive a long-term seasonal representation of the flows; a continuous description of the flows through time, with a periodicity of one year, is obtained by Fourier analysing the 12 monthly values for each river. The results of this analysis for $Q_{f,2\frac{1}{2}}$ are shown in figure 6; the maximum

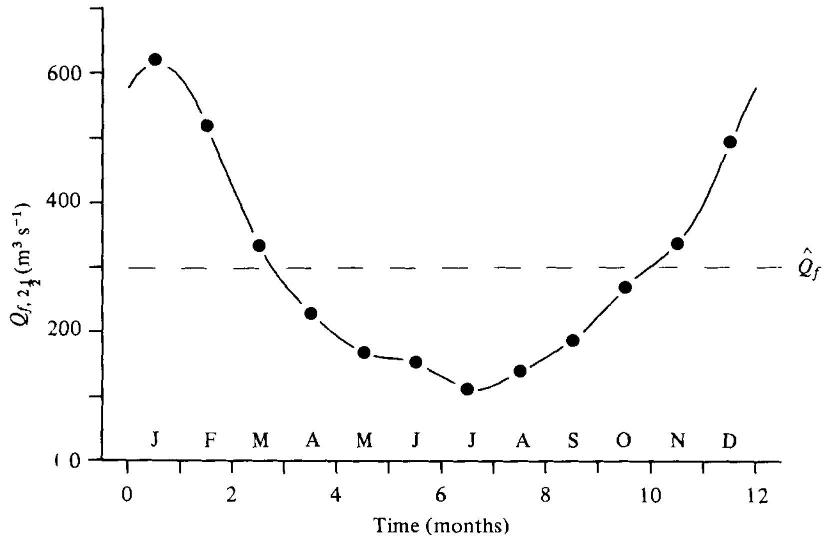

FIGURE 6. Long-term seasonal representation of freshwater inputs to the whole estuary, $Q_{f,2\frac{1}{2}}$, as a function of time. ●, monthly-averaged data for 1971–1976; ——, Fourier analysis of data; – – –, $\hat{Q}_f$.

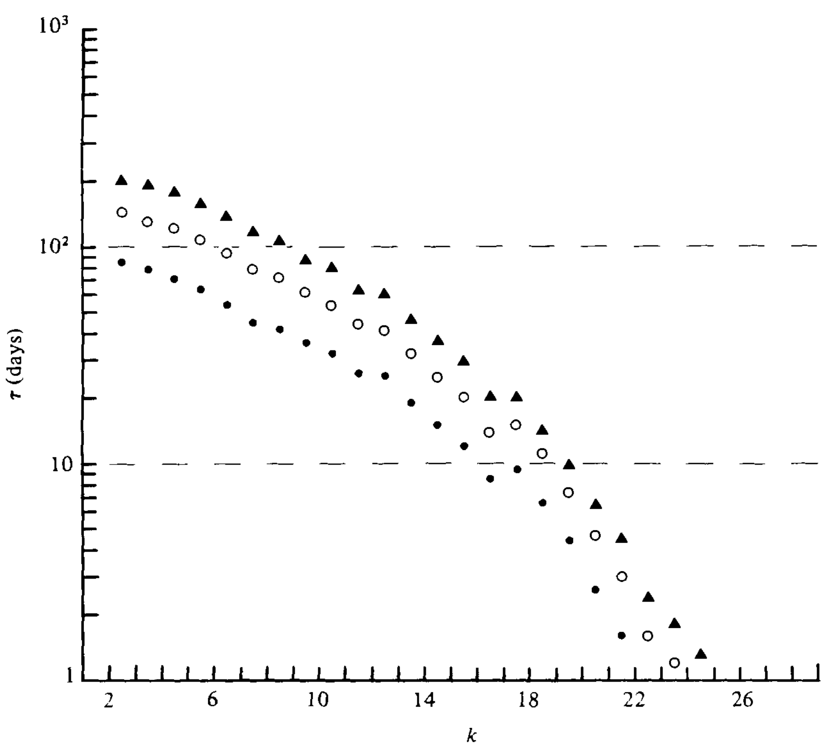

FIGURE 7. Seasonal variations in residence times, τ, as functions of k. ●, February; ▲, August; ○, yearly-averaged values of τ.

flow of roughly 600 $m^3 s^{-1}$ occurring in January, and the minimum flow of 100 $m^3 s^{-1}$ in July. Daily flows within a particular year will, of course, vary greatly from the main seasonal variations shown in figure 6. Equation (16) is solved until solutions having a periodicity of one year are reached; coefficients D_1, D_2 and D_3 are taken from table 2, and D is determined from equation (23) with $R = \hat{R}$ and with $Q^*_{f,2\frac{1}{2}}$ defined from figure 6 – the appropriate averaging periods, d^*, being given in table 1.

Residence times, τ, for February and August, together with the yearly-averaged values, are shown as functions of k in figure 7; τ has its maximum and minimum values during August and February respectively. The residence time for the whole estuary landward of Minehead increases from 90 days during February to 200 days during August, and has a yearly-averaged value of 140 days. These estimates are consistent with previously reported values of the flushing time for the Severn Estuary, based on the application of equation (28) to data from three IMER cruises (Institute for Marine Environmental Research 1975 p. 18); and also with a value of 160 days for the region between Newport and Porthcawl (located roughly 17 km seawards of Minehead) derived from data reported by Hamilton (Hamilton 1973, p. 416), and based on an average freshwater input of 300 $m^3 s^{-1}$.

Figure 7 shows that τ rapidly decreases towards the head of the estuary. For values of τ less than about one day (roughly landward of Newnham, see figure 1*b*) the rate of flushing of fresh water and dissolved materials is dominated by the tides and freshwater flows within the day; for values of τ less than about two weeks (roughly landward of the Severn Road Bridge, see figure 1*a*) the rate of flushing is strongly influenced by the freshwater flows over the period and the state of the spring–neap cycle, the dispersion being larger at spring tides than at neap tides, as shown in figure 5(*c*). Further seawards the tidal influences become integrated, owing to the long residence times, and the rates of flushing vary predominantly with season.

6. Discussion

The results presented here are of value from both practical and fundamental viewpoints. The computed dispersion coefficients, D, enable dynamic simulations of the Severn Estuary ecosystem and its water quality to be undertaken, and supply proving data for the validation of analytic dispersion theories to wide, vertically well-mixed estuaries in general, the results of which might be applicable to the Severn in the event of a modification to its tidal regime (HRS Severn Barrage Study 1976).

The main theoretical interest of this paper lies with the development of a practical method of deducing dispersion coefficients from salinity data, and with the demonstration that their behaviour with run-off is qualitatively similar to that expected from theoretical considerations (Smith 1980). Important features of the practical method are the use of regression analyses to combine large quantities of data, with subsequent reduction in errors, and the restriction of the time-scale for run-off dependence of D to be the same as that for salinity, thereby avoiding the steady-state assumption, which is seldom valid. An alternative practical method of evaluating D is through dynamic simulation of the salinity distributions, using equation (16), and optimizing D by trial and error comparisons of the computed solutions with observed data (Van Dam, Suijlen & Brunsveld Van Hulten 1976). This procedure poses a formidable parameter-fitting problem, and suffers from the practical difficulty that continuous salinity data are not generally available for seaward boundary conditions in equation (16); moreover, the method does not immediately parametrize D in terms of the known exogenous variables. We have preferred to use the regression method, and to verify the accuracy of our results by using the computed dispersion coefficients in equation (16), in order to ensure that good agreement exists between observed and predicted salinity distributions.

Data for the Severn show that D generally increases with increasing run-off (an exception being the values for $17.5 \leqslant k \leqslant 20.5$, tables 2 and 3, where the dependence on run-off is insignificant), and, away from the mouth, depend upon tidal range, showing a small decrease with increasing tidal range in the seaward part of the estuary, and a large increase with increasing tidal range towards the head. It is stressed that the data presented in table 2 for $k \geqslant 25.5$ are subjective estimates only. Application of the data to equation (16) shows that the residence time of the whole estuary varies from roughly 100 days during winter conditions, to 200 days during summer conditions, and, for a particular section, decreases rapidly as that section approaches the head of the estuary.

The increase in D with increasing run-off is consistent with the results of an analysis of shear dispersion for wide, vertically well-mixed estuaries by Smith (1980); the dependence of D on run-off near the mouth and head of the estuary is not significantly different from that predicted by theory, but is significantly weaker in the central reaches. The weaker dependence may be a consequence of Coriolis effects, but is more likely to be due to channel curvature or the influence of lateral inputs of fresh water; indeed, the large input of fresh water from the Wye at $k = 17.5$ (figure 1*a* and table 2) may be responsible for the anomalous behaviour of D with run-off in this region. It is emphasized that we are not suggesting that the theory presently available for wide, vertically well-mixed estuaries is capable of predicting the dispersion in a complex natural system such as the Severn, but merely demonstrating that qualitative similarities exist between theoretical results and observed data.

According to theory, the dependence of D on run-off is mainly due to the shearing effect of buoyancy-driven lateral circulation patterns; in this process, axial density gradients drive currents of higher salinity landwards in the deeper channels (where the effective frictional drag is smaller), and compensating currents of lower salinity seawards over the flanking shoals. In reality, the shear will be influenced by the large, but less organized, tidally induced residual currents resulting from channel and coastline curvature, and the strong, but localized, density gradients arising from lateral inputs of fresh water. The shearing effect of buoyancy-driven currents, and hence the dispersion, should decrease markedly at spring tides owing to increased lateral mixing. This is not observed; however, one consequence of the long residence times of the Severn is that, except near the head (see figure 7), spring–neap changes in salinity are very small, so that salinity is not an ideal indicator of such variability in the seaward part of the estuary. This does not invalidate our results for the spring–neap variations, but serves to emphasize that the results reflect only the observable influences of tidal variability in an estuary where the time-scales are generally greatly in excess of the spring–neap tidal period of 15 days. The large observed increases in D with tidal range near the head (where the spring–neap cycle can be resolved, $\tau < 7.5$ days) are probably a consequence of increasing estuarine volume at spring tides due to the Stokes drift (Uncles & Jordan 1980), and may even be enhanced by the formation of the Severn Bore for very high tides.

Each estuary has a unique topography, and hence a unique set of dispersion coefficients, although the observed increase in D with increasing run-off for the Severn also appears to be a feature of data for the Mersey, Thames and Tay (Bowden 1964, p. 337; Williams & West 1973, p. 123) and the Ems (Van Dam *et al.* 1976, p. 12.11). It is hoped that the presentation of these data for the Severn will motivate the presentation of similarly extensive data for other estuaries, the results of which will facilitate the development of analytic theories of dispersion.

This work, which forms part of the estuarine ecology programme of the Natural Environment Research Council, was partly supported by the Department of the Environment on Contract no. DGR 480/48, and is published with their permission.

REFERENCES

ABDULLAH, M. I., DUNLOP, H. M. & GARDNER, D. 1973 Chemical and hydrographic observations in the Bristol Channel during April and June 1971. *J. Mar. Biol. Ass.* **53**, 299–319.

ADMIRALTY TIDE TABLES, vol. 1 1978 The Hydrographer of the Navy, Hydrographic Department, Crossway, Taunton, Somerset, U.K.

BOWDEN, K. F. 1955 Physical oceanography of the Irish Sea. *Fishery Investigations* II **18** (8).

BOWDEN, K. F. 1964 The mixing processes in a tidal estuary. *Int. Conf. Water Pollution Res., London, September* 1962, pp. 329–346.

BOYLE, E., COLLIER, R., DENGLER, A. T., EDMOND, J. M., NG, A.C. & Stallard, R. F. 1974 On the chemical mass-balance in estuaries. *Geochim. & Cosmochim. Acta* **38**, 1719–1728.

DYER, K. R. 1974 The salt balance in stratified estuaries. *Estuarine & Coastal Mar. Sci.* **2**, 273–281.

FISCHER, H. B. 1972 Mass transport mechanisms in partially stratified estuaries. *J. Fluid Mech.* **53**, 671–687.

FISCHER, H. B. 1976 Mixing and dispersion in estuaries. *Ann. Rev. Fluid Mech.* **8**, 107–133.

HAMILTON, P. 1973 The circulation of the Bristol Channel. *Geophysical J. Roy. Ast. Soc.* **32**, 409–422.

HRS SEVERN BARRAGE STUDY 1976 *HRS Rep.* EX 753. Hydraulics Research Station, Wallingford, U.K.

INSTITUTE FOR MARINE ENVIRONMENTAL RESEARCH 1975 *Ann. Rep.* (1974–1975).

MOLLOWNEY, B. M. 1973 One-dimensional models of estuarine pollution. In *Mathematical and Hydraulic Modelling of Estuarine Pollution, Water Pollution Res. Tech. Paper* no. 13, 106–113.

O'CONNOR, D. J. 1962 Organic pollution of New York Harbor – theoretical considerations. *J. Water Pollution Control Fed.* **34**, 905–919.

PRITCHARD, D. W. 1954 A study of the salt balance in a coastal plain estuary. *J. Mar. Res.* **13**, 133–144.

RICHTMYER, R. D. & MORTON, K. W. 1967 *Difference Methods for Initial Value Problems*, 2nd edn. Tracts in Mathematics, vol. 4. Wiley-Interscience.

SMITH, R. 1977 Contaminants in small estuaries. *J. Fluid Mech.* **82**, 129–146.

SMITH, R. 1980 Buoyancy effects upon longitudinal dispersion in wide well-mixed estuaries. *Phil. Trans. Roy. Soc.* (To appear.)

STOMMEL, H. 1953 Computation of pollution in a vertically mixed estuary. *Sewage & Ind. Wastes* **25**, 1065–1071.

TALBOT, J. W. & TALBOT, G. A. 1974 Diffusion in shallow seas and in English coastal and estuarine waters. *Rapp. P.-V. Réun. Cons. Int. Explor. Mer* **167**, 93–110.

UNCLES, R. J. & JORDAN, M. B. 1979 Residual fluxes of water and salt at two stations in the Severn Estuary. *Estuarine & Coastal Mar. Sci.* **9**, 287–302.

UNCLES, R. J. & JORDAN, M. B. 1980 A one-dimensional representation of residual currents in the Severn Estuary and associated observations. *Estuarine & Coastal Mar. Sci.* **10**, 39–60.

VAN DAM, G. C., SUIJLEN, J. M. & BRUNSVELD VAN HULTEN, H. W. 1976 A one-dimensional water quality model based upon finite difference methods. In *Systems and Models in Air and Water Pollution*, §§ 12.1–12.11. Institute of Measurement and Control.

WILLIAMS, D. J. A. & WEST, J. R. 1973 A one-dimensional representation of mixing in the Tay Estuary. In *Mathematical and Hydraulic Modelling of Estuarine Pollution. Water Pollution Res. Tech. Paper* no. 13, 117–125.

WINTERS, A. 1973 A desk study of the Severn Estuary. In *Mathematical and Hydraulic Modelling of Estuarine Pollution. Water Pollution Res. Tech. Paper* no. 13, 106–113.

WINTERS, A. & BARRETT, M. J. 1972 Water quality in the Severn Estuary and recommendations for future investigations. *Water Pollution Res. Rep.* no. 1276.